Original Article

Synthesis, Characterization, and Cytotoxicity Evaluation of Polyethylene Glycol-Coated Iron Oxide Nanoparticles for Radiotherapy Application

Madhuri Anuje, Padmaja N. Pawaskar, Vishwajeet Khot, Ajay Sivan[1], Satish Jadhav, Jagruti Meshram, Balu Thombare[2]

Department of Medical Physics, Center for Interdisciplinary Research, D.Y. Patil Education Society (Deemed to be University), Kolhapur, [1]Department of Radiotherapy, Integrated Cancer Treatment and Research Centre, [2]Department of Physics, Savitri Bai Phule Pune University, Pune, Maharashtra, India

Abstract

Background: Treatment methods for cancer that are widely being utilized affect both normal and cancerous cells. We report synthesis polyethylene glycol (PEG)-coated Fe_3O_4 nanoparticles (NPs) and its characteristic properties and appraise its potential as a promising radiation sensitizer candidate in radiotherapy that improves cancer treatment and reduces side effects of radiation. **Materials and methods:** PEG-coated Fe_3O_4 NPs were synthesized by chemical coprecipitation method and characterized by studying their size, structure, functional group, stability, magnetization, and cytotoxicity using different techniques. X-ray powder diffraction, Fourier transform infrared spectroscopy, and thermogravimetric analysis results show that Fe_3O_4 NPs have been functionalized with PEG molecules during the course of synthesis. **Results:** Synthesized NPs have good stability based on zeta-potential study. Dynamic light-scattering results reveal that PEG-coated Fe_3O_4 has a greater hydrodynamic size than bare Fe_3O_4. Transmission electron microscopy (TEM) micrograph exhibited that NPs are roughly spherical with size in range of 10–20 nm. Saturation magnetization value of PEG-coated and bare Fe_3O_4 also confirms coating and shows superparamagnetic behavior. Cytotoxicity evaluation study indicated that PEG-coated Fe_3O_4 is biocompatible on L929 and toxic on Michigan Cancer Foundation-7 (MCF-7) (breast cancer cells). **Conclusion:** These characterized properties of PEG-coated Fe_3O_4 NPs show that it could be used as a potential radiosensitizer candidate in radiotherapy to significantly improve cancer treatment and minimize painful side effects of radiation.

Keywords: Fe_3O_4, MTT assay, polyethylene glycol, radiotherapy sensitizer

Received on: 17-10-2020 **Review completed on: 01-06-2021** **Accepted on: 01-06-2021** **Published on: 08-09-2021**

Introduction

Control of cancer is considered to be a foremost communal health issue in prevalent time. As per the World Health Organization report, cancer is the second leading cause of death globally, and has caused an estimated 9.6 million deaths in 2018 itself. Globally, about 1 of 6 deaths relates to cancer.[1] Increasing morbidity and fatality due to cancer negatively affects the financial and overall growth of the nation. Cancer can be treated with various treatment methods including chemotherapy, radiation therapy, immunotherapy, and surgery. Radiotherapy still remains one of the most effective methods for the treatment of primary and metastatic tumors, microscopic tumor spread as well as regional lymph nodes.[2] In radiotherapy, tumor cells are killed by high-energy X-rays or gamma-rays. In case of deep-seated tumor, healthy tissues that lie in track of photon get exposed to radiation resulting into severe side effects. The main challenge that radiation oncologists and medical physicists facing is that how to minimize normal tissue dose at the same time increasing dose impact on the tumor tissue. To achieve this goal of radiotherapy, technological advances such as new imaging modalities, more powerful computer hardware as well as software and new delivery systems like advanced linear accelerators have been used. However, increasing the radiation dose is still insufficient to significantly improve tumor control probability for many

Access this article online

Quick Response Code:

Website: www.jmp.org.in

DOI: 10.4103/jmp.JMP_102_20

Address for correspondence: Dr. Padmaja N. Pawaskar, Department of Medical Physics, Center for Interdisciplinary Research, D.Y. Patil Education Society (Deemed to be University), Kolhapur - 416 006, Maharashtra, India.
E-mail: samgrish@gmail.com

How to cite this article: Anuje M, Pawaskar PN, Khot V, Sivan A, Jadhav S, Meshram J, *et al*. Synthesis, characterization, and cytotoxicity evaluation of polyethylene glycol-coated iron oxide nanoparticles for radiotherapy application. J Med Phys 2021;46:154-61.

radioresistant tumors.[2,3] Another challenge for radiotherapy is that tumors are often located near normal tissue and organs at risk which is a limiting factor for radiation to deliverer.[2] Therefore, increasing radiosensitization of tumor tissue with the use of radiosensitizers has attracted great interest in radiation oncology.[2] Currently, chemotherapeutics are being used in conjunction with radiation therapy to increase its effectiveness. The application of chemical agents that simply have an additive effect on normal tissues is equivalent to the administration of an increment of radiation dose with no differential benefit.[4] The toxicity impact of both chemical agents and radiation therapy overlap resulting into minimal therapeutic gain.[4] Hence, it is necessary to focus on biocompatible radiosensitizer with minimum side effects to normal tissue.

Nanomaterials with well-developed synthetic methods, low cytotoxicity, good biocompatibility, and ease of functionalization are promising for use as radiosensitizers.[5] Nanoparticles (NPs) have smaller size, more cell penetration rate, and fewer adverse effects than conventional radiosensitizers and at the same time have enhanced permeability and retention effect.[6] Among nanomaterials which have this radiosensitizing nature, carbon nanotubes, gold NPs, and other metallic NPs can be mentioned.[6] Typically, iron oxide NPs are commonly used for biomedical applications such as contrast agent in magnetic resonance imaging, colloidal mediator for cancer magnetic hyperthermia,[7] targeted drug deliverer, and in cell separation techniques.[8] They are extensively used in diagnostics and therapies of cancer treatment due to their peculiar and essential properties such as excellent biocompatibility, superparamagnetic behavior,[8] physico/chemical stability, environmental safety, and ease of synthesis process with surface treatment.[9] When superparamagnetic iron oxide NPs (SPIONs) reach smaller sizes (about 10–20 nm for iron oxide), superparamagnetic properties become evident, so that the particles reach a better performance for most of the aforementioned applications.[10] Superparamagnetic behavior enables to guide SPIONs to tumor area by using external inhomogeneous magnetic field while biocompatibility allows for their medical application.[8] SPIONs can be formed in three natural types such as hematite (α-Fe_2O_3), maghemite (γ-Fe_2O_3), and magnetite (Fe_3O_4; iron (II, III) oxide).[9] Based on cytotoxicity evaluation and its composition, Fe_3O_4 is found to be cytotoxic as it contains Fe^{2+} ions and helps in the formation of reactive oxygen species (ROS) such as hydroxyl radical, superoxide anion, hydrogen peroxide, and hydroperoxyl radical (e.g., $OH^{\cdot}$, O_2^{-}, H_2O_2, $HO_2^{\cdot}$), which provides oxidative stresses.[8] The pathway of production of ROS is the Haber–Weiss reaction which results in the generation of the highly reactive hydroxyl radical from the reaction between superoxide and hydrogen peroxide.[11]

Efficacy of radiation can be increased with the use of iron oxide NPs as a sensitizer due to their ability to produce ROS. Radiation therapy promotes leakage of electrons from the electron transport chain and leads to an increase in mitochondrial production of the superoxide anion which is converted to hydrogen peroxide by superoxide dismutase. Iron oxide NPs can then catalyze the reaction from hydrogen peroxide to the highly reactive hydroxyl radical.[11]

When a foreign body such as NPs enters into the bloodstream, serum proteins known as opsonin recognize and adsorb it for clearance from the body.[12] This can be prevented by biocompatible coating of NPs. Biocompatible coating improves stability by avoiding agglomeration of NPs. Furthermore, to reach the specific site of interest, NPs should have long circulation time. Layer of hydrophilic coating creates a cloud of chains at the surface of NP and causes steric repulsive forces against plasma proteins and increases the blood circulation half-life of targeted nanocarriers.[13] Hydrophilic-coated NPs can be fabricated by making use of polymer types such as PEG, PEG-based copolymers, and polyvinylpyrrolidone.[13] PEG-coated NPs have been reported to have a half-life over 7 h, while in the absence of PEG, it is less than minute.[14] Furthermore, increasing amount of PEG on NP surface increases blood circulation time. PEG can act as lubricant and binder, nontoxic, and antibacterial.[15] Smaller size NPs have enhanced permeability and retention effects such that they can easily accumulate within tumor region with even distribution.[14] As particle size deceases, the surface atoms greatly increase with decreasing atomic coordination number.[16] Shape plays a crucial parameter in determining the behavior of NPs in various processes including blood circulation, targeting, cellular uptake, and intracellular trafficking.[14] Gratton *et al*. experimentally demonstrated that particles with higher aspect ratios facilitate cellular uptake in cancer cells.[17] The benefits of nonspherical shapes in targeting and internalization have been suggested in theoretical model.[18]

When radiation interacts with NPs, electrons get ejected by photoelectric and Compton effect. Interaction of these electrons may be direct or indirect. In the indirect action, these electrons produce ROS which, in turn, attack DNA to kill cancer cell. About two-thirds of the biologic damage by radiation is caused by indirect action.[19] ROS production by SPIONs and radiation enhances the therapeutic efficiency of radiotherapy.

In this study, PEG-coated Fe_3O_4 NPs were synthesized by chemical coprecipitation method and characterized by X-ray powder diffraction (X-RD), Fourier transform infrared spectroscopy (FTIR), thermogravimetric analysis (TGA), zeta-potential measurements, dynamic light scattering (DLS), transmission electron microscopy (TEM), and vibrating sample magnetometer (VSM). Cytotoxicity study has been carried out in order to assess tumor cell killing as well as normal cell biocompatibility.

Experimental Procedure

Synthesis and characterization of polyethylene glycol-coated and uncoated Fe_3O_4

Materials

Iron (III) chloride anhydrous ($FeCl_3$, 96%), ferrous chloride hydrated ($FeCl_2$, 98%), potassium hydroxide pellets (KOH),

and polyethylene glycol (PEG 400) were purchased from Sigma-Aldrich. All these chemicals were used directly without further purification.

Synthesis of polyethylene glycol-coated and uncoated Fe_3O_4 nanoparticles

A facile chemical coprecipitation method was used to synthesis bare Fe_3O_4 and PEG-coated Fe_3O_4 NPs.[15] This simple cost-effective and efficient method provides a pathway to control the composition, shape, and size of NPs. Bare Fe_3O_4 was synthesized by adding droplet wise a base 1 M of KOH (1 M of KOH pellets dissolved in 100 ml distilled water) solution to an aqueous mixture of Fe^{2+} and Fe^{3+} chloride with a 1:2 molar ratio for 45 min to obtain homogeneous solution. Temperature was maintained at 90°C with stirring rate of 1100 rpm in the continuous flow of inert nitrogen gas to avoid the oxidation of NPs that also help to reduce size, resulting in black color precipitate at the bottom. Precipitate was magnetically separated using permanent magnet and washed several times gently and kept in oven at 90°C for 12 h. PEG-coated Fe_3O_4 was synthesized by adding 10 ml PEG 400 to an aqueous mixture of Fe^{2+} and Fe^{3+} chloride with 1:2 molar ratio and then by adding droplet wise a base 1 M of KOH (1 M of KOH pellets dissolved in 100 ml distilled water) solution for 45 min to obtain homogeneous solution. Temperature was maintained at 90°C with a stirring rate of 1100 rpm to functionalize and stabilize iron oxide NPs. Temperature was maintained at 90°C with a stirring rate of 1100 rpm. The solution appears black in color. When required condition for precipitation was achieved, solution allowed settling down. Precipitate was magnetically separated using permanent magnet and washed several times gently and kept in oven at 90°C for 12 h.

Characterization

The X-ray diffraction patterns of bare Fe_3O_4 and PEG-coated Fe_3O_4 NPs were performed on an X-ray diffractometer (Rigaku MiniFlex -600). The infrared spectra were recorded in the range of 4000 to 500 cm^{-1} on a Fourier transform infrared spectrometer (Jasco FTIR-6100). Thermal gravimetric analysis was performed by TA instruments Lab Q50 under nitrogen gas atmosphere from 300°C to 600°C with heating rate of 10°C/min. Zeta-potential was carried out on a 90 plus particle size analyzer, Brookhaven, USA. DLS for hydrodynamic size determination was performed on Zetasizer, Malvern Instruments Ltd. Two milligrams of PEG-coated NPs was dissolved in 2 ml of distilled water and sonicated for 2–3 min. Supernatant of the solution was taken to study hydrodynamic size. NP size was determined by transmission electron micrograph taken on JEOL JEM-2100F field emission gun transmission electron microscope (HR-TEM). The magnetic property of PEG-coated Fe_3O_4 NPs was measured using EG and GPAR 4500 VSM at 300 K.

***In vitro* cytotoxicity study of polyethylene glycol-coated and uncoated Fe_3O_4 nanoparticles**

Materials

L929 mouse fibroblast and MCF-7 breast cancer cell, Dulbecco's Modified Eagle's Medium (DMEM, HiMedia) containing 10% fetal bovine serum (FBS, Thermo Fisher Scientific), Neubauer's chamber, 96-well tissue culture-treated plate, EZcount MTT Cell Assay Kit (HiMedia), phosphate-buffered saline (Thermo Fisher Scientific), T25 flasks (Thermo Fisher Scientific), Nalgene syringe filter (0.2 µm PES, Thermo Fisher Scientific). Culture flasks were incubated in a CO_2 incubator at 37°C with 5.0% CO_2. All experiments were carried out in triplicate. The cell survival value among the different groups was compared using two-tailed unpaired *t*-test with a $P \leq 0.05$ considered statistically significant.

Cell culture

10^4 cells/well was added in a 96-well tissue culture-treated plate (cell count was taken on a Neubauer's chamber). The plate was incubated at 37°C in a 5% CO_2 incubator for 24 h. After 24-h incubation, the plate was observed under inverted microscope to check the morphology of the cells and confluency of the wells in the 96-well plates. Sterile test sample was suspended in DMEM containing 10% FBS at a known concentration, and dilutions for the same were made accordingly. One hundred microliters of each of the test samples of different concentrations was added along with the positive control (doxorubicin) and normal control (cells with medium and no test sample). In post sample addition, the plate was incubated at the same 37°C in a 5% CO_2 incubator for 24 h. After 24-h incubation, the plate was observed under the inverted microscope and photographs were taken of the recorded observations. Test sample was removed, and 90 µl fresh DMEM containing 10% FBS was added. Then, 10 µl of MTT reagent was added to each well. The plate was wrapped in aluminum foil and incubated at 37°C in a 5% CO_2 incubator for 4 h. In post 4-h incubation, the entire medium was removed by flicking the plate and 100 µl of solubilization buffer was added to each well and incubated at 37°C in a 5% CO_2 incubator for about 20 min. Post incubation, absorbance was measured at 570 nm and 630 nm on a 96-well plate reader.[8]

Results and Discussion

Structural analysis

X-ray diffraction

The X-ray diffraction (X-RD) pattern was obtained of synthesized bare Fe_3O_4 and PEG-coated Fe_3O_4 NPs were characterized by X-RD technique using Rigaku MiniFlex-600 (CuKα, λ=1.5406Aº radiation) and X-RD was taken every time to confirm its structure. Size of nanoparticles was calculated for high intense peak of 311 using Scherer's relation (3) as

$$D = \frac{K\lambda}{\beta cos\theta} \text{(III)}$$

Where β is the full width at half maxima, K is a shape factor constant (0.91), and λ is the wavelength of Cu-Kα X-ray source (1.5406 A°) and is found in the range of 8–12 nm. The X-RD pattern reveals the formation of single-phase PEG-coated Fe_3O_4 and uncoated Fe_3O_4, NPs with a = 8.3952 A°.

The crystalline size of PEG-coated Fe_3O_4 and bare Fe_3O_4 is estimated to be about 9.86 nm and 10.94 nm, respectively; X-ray line broadening reveals that coating reduces peak intensity and decreases the crystalline size of NPs.[15] Figure 1 shows that the diffraction peaks at 2 θ =30.36°, 35.72°, 43.44°, 57.26°, and 62.92° can be assigned to the 220, 311, 400, 333, and 440 planes, respectively, indicating cubic crystal structure of pure Fe_3O_4. Figure 1 clearly shows that diffraction peaks for uncoated Fe_3O_4 [Figure 1a] are stronger in intensity and narrower as compared to PEG-coated Fe_3O_4 [Figure 1b]. It shows that crystallinity decreases for coated NPs.[15]

Fourier transform infrared spectrometry

The FTIR spectra of bare Fe3O4, PEG-coated Fe3O4 NPs, and PEG are shown in Figure 2. The presence of PEG biocompatible coating on PEG-coated Fe3O4 NPs has been analyzed by detailed FTIR studies, as shown in Figure 2 and in Table 1. FTIR analysis was carried out in the range of 500 cm^{-1}–4000 cm^{-1} wave number interval. The data plot transmits the wave number of infrared light in the form of sharp absorption peaks at peculiar certain wave numbers resulting from the vibration of certain functional groups. In PEG spectra [Figure 2c], absorption peak seen at 1092.6 cm^{-1} is due to C-O-C ether stretch band.[21] -CH_2 bending bands are appeared at 1453.40 cm^{-1} and 1249.3 cm^{-1}. The peak at 940.09 cm^{-1} corresponds to the out-of-plane bending vibration of -CH band.[21] Infrared wave number absorption occurred at 2867.6 cm^{-1} is due to -CH stretching vibration band.[22] In pure Fe_3O_4 spectrum [Figure 2a], it is identified that the occurrence of bending vibration of H-O-H at 1634.3 cm^{-1} is due to adsorbed water.[20] Stretching vibration of Fe-O functional group occurs for absorption of infrared wave number at 603.61 cm^{-1}. In PEG-coated Fe_3O_4 FTIR spectra [Figure 2b], the main absorbance of ether stretch band is seen at 1098.2 cm^{-1}. Bending vibrations of -CH_2 and -CH band are seen at 1460.08 cm^{-1}, 1251.5 cm^{-1}, and 951.69 cm^{-1}, respectively. Furthermore, H-O-H bending is seen around 1644.9 cm^{1}. Fe-O vibration in PEG-coated appeared around 677.85 cm^{-1}. The broad peak in between 3400 and 3028 cm^{-1} in all of these spectra of PEG, PEG coated, and iron oxide belongs to attached hydroxyl group [Table 1].[20] The presence of C-O-C ether stretch, -CH bending, H-O-H bending, and Fe-O stretching vibrational anomalies in PEG-coated Fe_3O_4 confirms that Fe_3O_4 is coated with PEG on its surface.

Thermal gravimetric analysis

Figure 3 shows the thermogravimetric analysis of bare Fe_3O_4 and PEG-coated Fe_3O_4 NPs. TGA curve shows that decomposition of PEG coat (curve 3b) of NPs started around 194°C and ended around 375°C. Indicating the total weight loss of 18.13% results from decomposition of PEG polymers from the surface of PEG-coated Fe_3O_4 NPs. From uncoated Fe_3O_4 (curve 3a), it is seen that decomposition started around 179°C and percentage weight loss is about 10.4%. The increment in onset decomposition temperature about 15°C of PEG-coated NPs and difference in percentage weight loss confirms the strong attachment of PEG molecules on surfaces of Fe_3O_4 NPs.

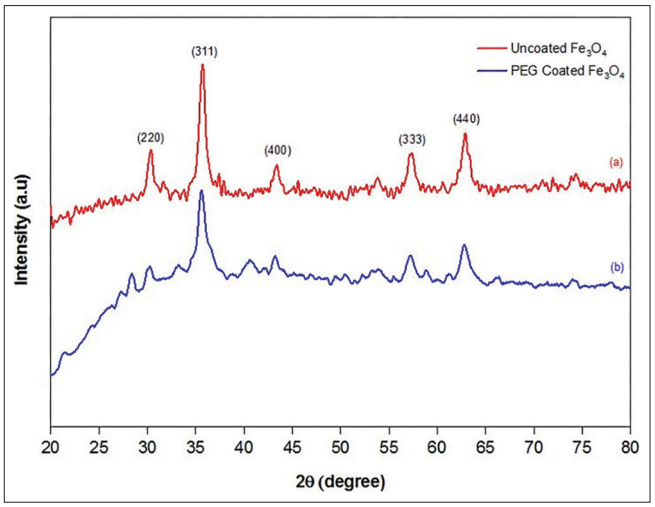

Figure 1: X-ray powder diffraction spectra of (a) uncoated Fe_3O_4 and (b) polyethylene glycol-coated Fe_3O_4

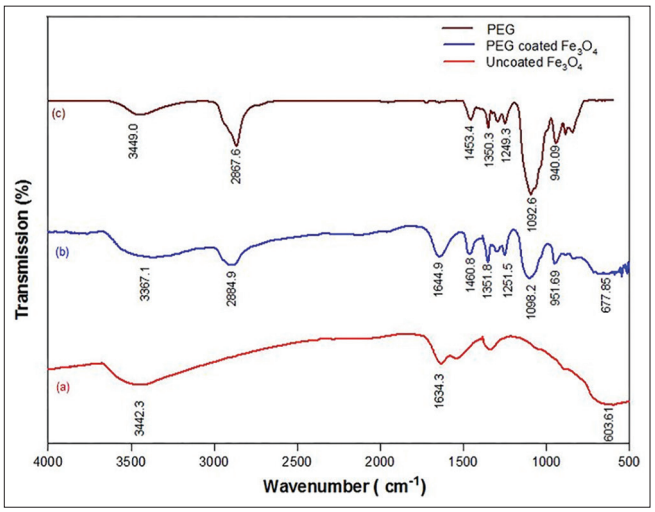

Figure 2: Fourier transform infrared spectroscopy spectra of (a) uncoated Fe_3O_4, (b) polyethylene glycol-coated Fe_3O_4, and (c) polyethylene glycol

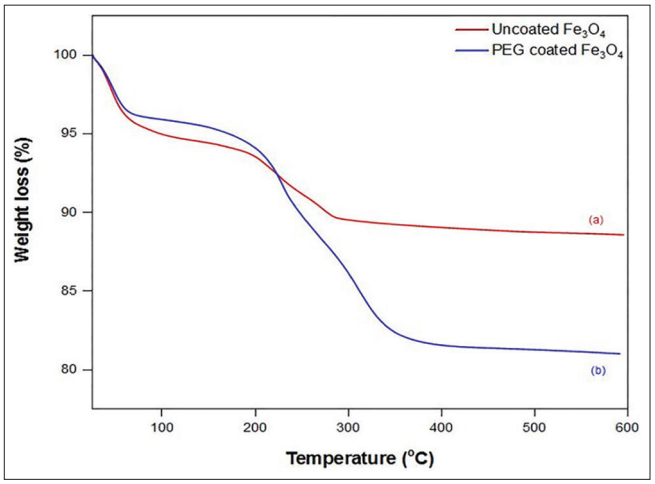

Figure 3: Thermogravimetric analysis curves of uncoated Fe_3O_4 (a) and polyethylene glycol-coated Fe_3O_4 (b)

Table 1: Functional group bonds of Fe_3O_4 nanoparticles[20]

Wave number (cm^{-1})	Functional group
658-506	Fe-O stretching
1672-1367	H-O-H bending
3400-3028	O-H stretching
2920-2855	C-H stretching

Colloidal stability study

Zeta-potential measurements

Higher colloidal stability of the NPs is due to stronger charge on surface and hence will lead to longer shelf life.[23] Colloidal stability of PEG-coated Fe_3O_4 was studied by zeta-potential measurements. The average zeta-potential value for PEG-coated Fe_3O_4 was found to be 32.65 mV.[24] Under the applied electric field, the specimen particles dissolved move toward the electrode of opposite charge. The intensity fluctuations of the laser light scattered by the sample particles proportional to their electrophoretic mobility (velocity) are transformed into the zeta-potential values. Zeta-potential value determines the stability of colloidal systems. Colloidal systems with zeta-potential higher than 30 mV are strongly charged and become stable due to particle–particle repulsion, thus avoiding agglomeration of particles and provides control over the size of NPs.

Dynamic light scattering

The size of PEG-coated Fe_3O_4 in water was studied by DLS, which is a useful parameter to decide blood half lifetime and biodistribution of NPs. The greater amount of PEG coverage increases the blood circulation time.[14] Here, 10 ml of PEG 400 concentration used during synthesis showed hydrodynamic size around 342–396 nm, as shown in Figure 4b. This may be due to the formation of extended hydrogen bond networks between ethylene groups present on the surface of NPs and water molecules in neighborhood. In all the cases, the hydrodynamic sizes are higher as compared to particle size obtained from XRD and TEM. The higher diameter value obtained in DLS measurement may be due to aggregation and contribution from solvent molecules being adsorbed on particle surface, surfactant layer and canted surface.[25] Hydrodynamic size for uncoated Fe_3O_4 is about 229–265 nm [Figure 4a]. For coated NP, hydrodynamic size is greater due to the presence of PEG on Fe_3O_4.

Morphological study

High-resolution transmission electron microscopy

High-resolution TEM (HR-TEM) study was carried for PEG-coated Fe_3O_4 NPs to have the detailed information about size, shape, structure, and morphology of the NPs. HR-TEM images, Figure 5a-e of PEG-coated Fe_3O_4 NPs, exhibit polygonal structure with the size distribution between 10 and 20 nm. TEM micrographs of Fe_3O_4 NPs exhibit well-defined and homogeneous roughly spherical shape. This may be due to the PEG coating acting as a stabilizer and dispersing agent. Particle diameter was calculated by Image J software,

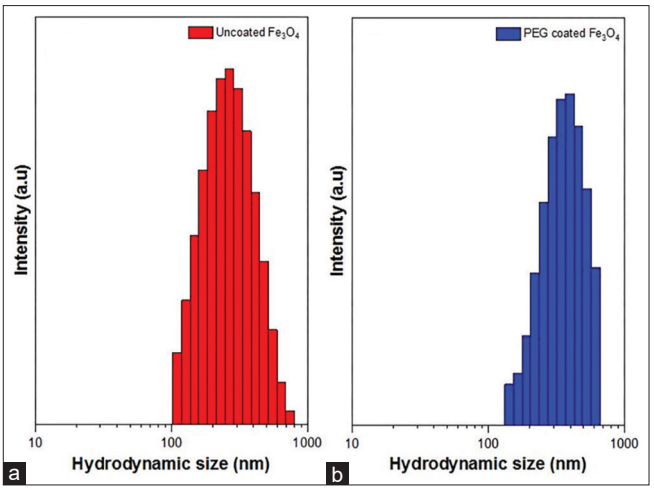

Figure 4: Hydrodynamic size of uncoated Fe_3O_4 (a) and polyethylene glycol-coated Fe_3O_4 (b)

which is in consistent with particle size calculated by X-RD results ($d_{X\text{-}RD}$ = 9.86 nm). The selected area electron diffraction pattern [Figure 5f] shows only diffraction intensity associated with crystalline Fe_3O_4 which is similar to X-RD result.

Magnetization Study

Figure 6 shows the magnetic field versus magnetic moment (M − H) curve for bareFe_3O_4 and PEG-coated Fe_3O_4 NPs exhibiting superparamagnetic behavior with zero coercivity (C_e) and zero remanence (M_r). The magnetic NPs in magnetic field get agglomerate due to magnetic dipole attraction and will be reduced after removal of magnetic field resulting in no residual magnetization before and after removal of magnetic field.[26] This superparamagnetic behavior of magnetic NPs is preferred for biomedical applications. This fact of nonexistence of coercive forces and remanence prevents magnetic dipolar interactions between NPs and their aggregation, which could lead to serious adverse problems such as the formation of clots in the blood circulation system.[27] Saturation magnetization values from graph for PEG-coated [Figure 6b] and bare Fe_3O_4 [Figure 6a] are about 34 emu/g and56 emu/g, respectively, which are smaller than theoretical value of bulk Fe_3O_4 (M_s = 92 emu/g) since M_s decreases with decreasing particle size[26] ($d_{X\text{-}RD}$ values for PEG-coated Fe_3O_4 = 9.86 nm and Fe_3O_4 = 10.94 nm). It has been reported that for biomedical application, M_s of 7–22 emu/g is adoptable.[28,29] The achieved M_s value of 34 emu/g for PEG-coated Fe_3O_4 NPs is acceptable for biomedical applications.

Cytotoxicity Study

Cell viability study has been carried out of PEG 400-coated and uncoated Fe_3O_4 for four different concentrations 0.1 mg/ml, 0.15 mg/ml, 0.2 mg/ml, and 0.25 mg/ml for both L929 normal and MCF-7 cancer cell lines. Micrographs were taken during experiment, as shown in Figure 7. Liu *et al*.

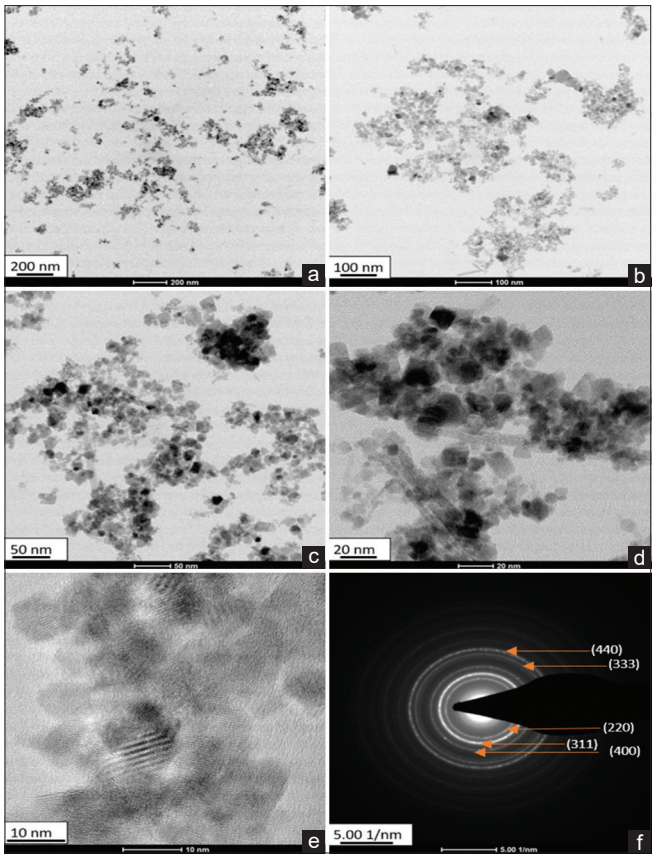

Figure 5: HR transmission electron microscope micrographs of polyethylene glycol-coated Fe_3O_4 nanoparticles of resolution 200 nm (a), 100 nm (b), 50 nm (c), 20 nm (d), 10 nm (e), and SAED pattern (f) of polyethylene glycol-coated Fe_3O_4

studied on biocompatibility of PEG derivatives on L929 cell lines and PEG-1000 and PEG-4000 are found moderate cytotoxic to L929 while PEG-400 and PEG-2000 nearly non-cytotoxic. Making PEG-400 a suitable coating candidate for the cytotoxicity study in agreement with our findings.[30] In this study, as concentration increases, cell viability decreases, as shown in Figure 8, while 0.25 mg/ml concentrations of both the NPs show greater toxicity in both the cell lines.On MCF-7 cell line, 78% killing was observed for 0.25 mg/ml PEG-coated Fe3O4 NPs whereas in the case of doxorubicin for 0.01 mg/ml it shows 86% cell killing. Doxorubicin shows the cytotoxic effect on cancer cell line as well as normal cell line which confirms drug has a side effect on normal tissue along with better tumor control.

It has been observed that PEG-coated Fe3O4 showing greater cell viability compared to bare Fe3O4 in both L929 and MCF 7 cell lines ($P < 0.05$), but L929 cell line has a greater percentage of viability compared to MCF 7 which shows that PEG coated Fe3O4 are more biocompatible [Figure 8e and f]. In the present study percentage of cell killing for MCF-7 was observed for 0.1 0.15 0.2 and 0.25 mg/ml to be 45.67, 51.3, 65.23, and 78.56%, respectively, while for L929 cell line they are 44.33, 46.44, 49.49, and 55.67% respectively with PEG coated Fe3O4 NPs. It shows that there is higher cell killing observed for MCF-7

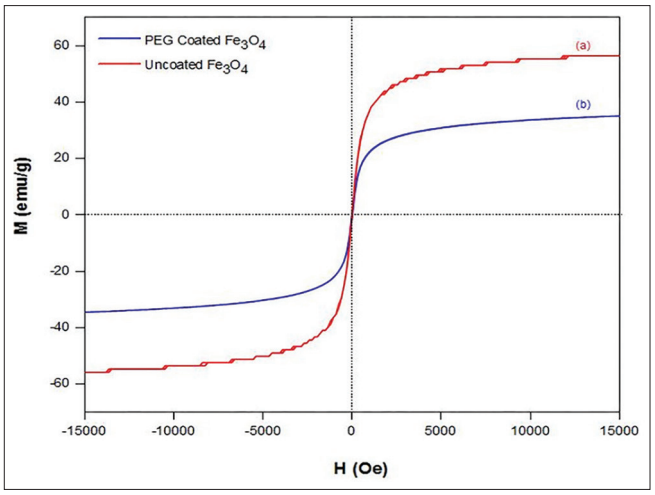

Figure 6: Magnetization curve for uncoated Fe_3O_4 (a) polyethylene glycol-coated Fe_3O_4 (b)

compared to L929 cell lines, especially for 0.2 and 0.25 mg/ml. For MCF-7 cancer cell lines, the percentage of killing observed for uncoated Fe_3O_4, for 0.1 mg/ml, 0.15 mg/ml, 0.2 mg/ml, and 0.25 mg/ml is about 55.67%, 61.34%, 66.67%, and 85%, respectively, while for L929 cell lines, it is 55.67%, 59.8%, 68.04%, and 75.26%, respectively. It shows that there is not much difference in cell killing for uncoated Fe_3O_4 for MCF-7 and L929 cell lines except 0.25 mg/ml.

From these studies, it has been observed that PEG-coated Fe_3O_4 NP (0.25 mg/ml) has a nearly equivalent cytotoxic effect on MCF-7 cancer cell lines and is biocompatible on L929 cell lines as compared to the standard drug (0.001 mg/ml). ROS production for cancer cell killing further may enhance while it is used as a radiosensitizer.

Conclusion

The main goal of radiotherapy is to increase the sensitivity of tumor in order to kill effectively while minimizing normal tissue dose. This can be achieved by using PEG-coated Fe_3O_4 NPs. Due to radiation exposure, surface coverage containing PEG may partially or fully destroy. Hence, Fe^{2+} ions are easily accessible and act as a more efficient catalyst by taking part in Haber–Weiss reaction for production of ROS species to enhance the radiation treatment of cancer therapy. In this review, we briefly summarize the synthesis, characterization, and cytotoxicity study in order to assess whether PEG-coated Fe_3O_4 NP is a suitable candidate as a radiotherapy sensitizer. Findings of size, shape, stability, and superparamagnetic behavior are observed to be much suitable for biomedical applications. XRD and TEM study shows that size of the nanoparticles is in the range of 8 to 20 nm. Also, FTIR, TGA and DLS studies confirms PEG coating of Fe_3O_4 NPs. Zeta potential and VSM studies show their stability and superparamagnetic behavior.

In cytotoxicity study, the percentage of cell killing observed for PEG-coated Fe_3O_4 is higher for MCF-7 compared to L929,

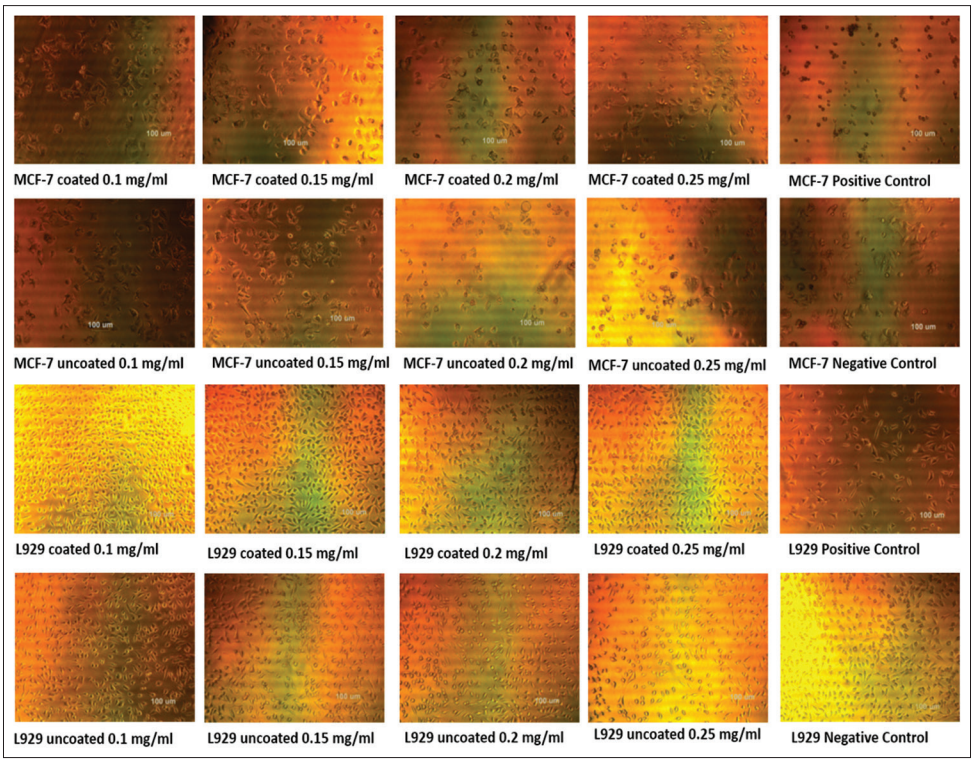

Figure 7: Micrographs taken during the experiment

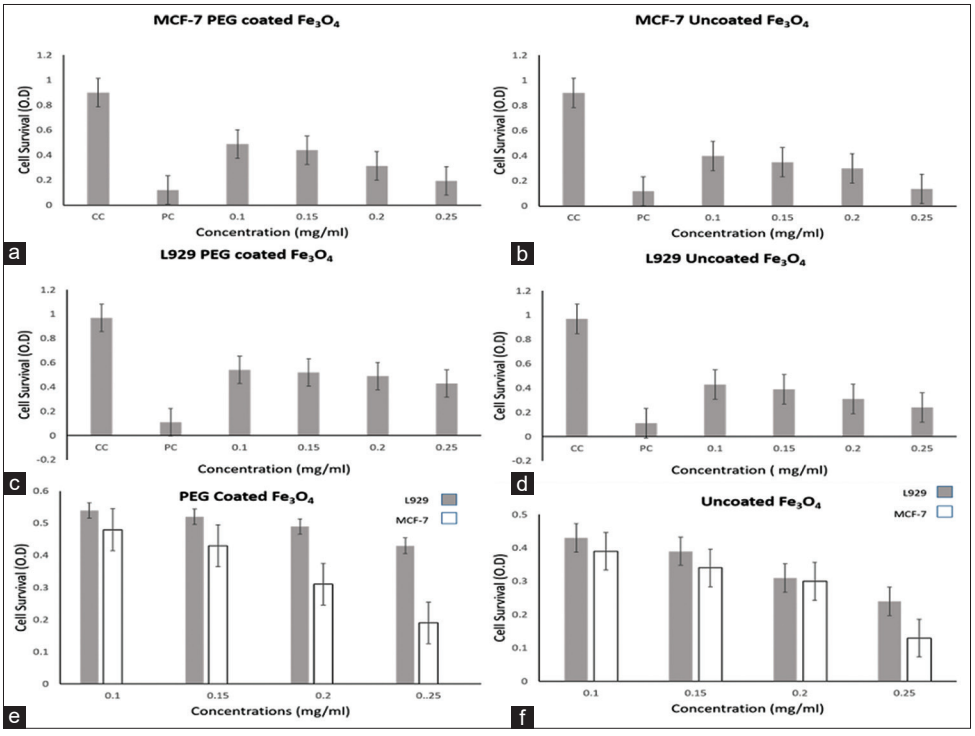

Figure 8: Concentration-dependent cytotoxicity of polyethylene glycol-coated Fe_3O_4 on MCF-7 (a) and uncoated Fe_3O_4 on MCF-7 (b). Concentration-dependent cytotoxicity of polyethylene glycol-coated Fe_3O_4 on L929 (c) and uncoated Fe_3O_4 on L929 cell lines (d). Comparison study of concentration-dependent cytotoxicity effect of polyethylene glycol-coated Fe_3O_4 on L929 and MCF-7 cell line. (e) And effect of uncoated Fe_3O_4 on L929 and MCF-7 cell lines. (f). It is observed that reduction in percentage of cell survival for MCF-7 compared to L929 was 5.1%, 8.1%, 17.7%, and 23.7% for concentrations 0.1, 0.15, 0.2, and 0.25 mg/ml, respectively, for polyethylene glycol-coated Fe_3O_4 (e). It is observed that reduction in percentage of cell survival for MCF-7 was 3.1%, 4.2%, 1%, and 10.5% for uncoated Fe_3O_4 (f)

this shows it is biocompatible. The percentage of cell killing observed for both MCF-7 and L929 is greater for bare Fe_3O_4 compared to PEG-coated Fe_3O_4. In all cases, 0.25 mg/ml concentration shows higher cell killing. Here, coating improves the biocompatibility nature of NPs, which makes it an appropriate contender. Overall, PEG-coated Fe_3O_4 can act as a radiosensitizer in radiotherapy which may promote new opportunities for progress in cancer radiotherapy to improve clinical efficacy in different cancer.

Financial support and sponsorship

Nil.

Conflicts of interest

There are no conflicts of interest.

References

1. Available from: https://www.who.int/news-room/fact-sheets/detail/cancer. [Last accessed on 2020 Jul16].
2. Liu Y, Zhang P, Li F, Jin X, Li J, Chen W, Li Q. Metal based Nano Enhancers for future radiotherapy: Radiosensitizing and synergistic effects on tumor cells. Theranostics, 2018;8:1824-49.
3. Baskar R, Lee KA, Yeo R, Yeoh KW. Cancer and radiation therapy: Current advances and future directions. Int J Med Sci 2012;9:193-9.
4. Koch CJ, Parliament MB, Brown JM, Urtasun RC. Chemical modifiers of radiation response. In: Hoppe RT, Phillips TL, Roach M, editors. Leibel and Phillips Textbook of Radiation Oncology. 3rd ed., Ch. 4. Philadelphia: W.B. Saunders; 2010. p. 55-68.
5. Wang H, Mu X, He H, Zhang XD. Cancer Radiosensitizers. Trends Pharmacol Sci 2018;39:24-48.
6. Babaei M, Ganjalikhani M. The potential effectiveness of nanoparticles as radio sensitizers for radiotherapy. Bioimpacts 2014;4:15-20.
7. Salunkhe AB, Khot VM, Pawar SH. Magnetic hyperthermia with magnetic nanoparticles: A status review. Curr Top Med Chem 2014;14:572-94.
8. Klein S, Sommer A, Distel LV, Neuhuber W, Kryschi C. Superparamagnetic iron oxide nanoparticles as radiosensitizer via enhanced reactive oxygen species formation. Bio Chem Biophys Res Commun 2012;425:393-7.
9. Ghazanfari MR, Kashefi M, Shams SF, Jaafari MR. Perspective of Fe3O4 nanoparticles role inbiomedical applications. Biochem Res Int 2016;2016:32.
10. Arias LS, Pessan JP, Vieira AP, Lima TM, Delbem AC, Monteiro DR. Iron oxide nanoparticles for biomedical applications: A perspective on synthesis, drugs, antimicrobial activity, and toxicity. Antibiotics (Basel) 2018;7:46.
11. Hauser AK, Mitov MI, Daley EF, McGarry RC, Anderson KW, Hilt JZ. Targeted iron oxide nanoparticles for the enhancement of radiation therapy. Biomaterials 2016;105:127-35.
12. Haume K, Rosa S, Grellet S, Śmiałek MA, Butterworth KT, Solov'yov AV, *et al.* Gold nanoparticles for cancer radiotherapy: A review. Cancer Nanotechnol 2016;7:8.
13. Murugan K, Choonara YE, Kumar P, Bijukumar D, du Toit LC, Pillay V. Parameters and characteristics governing cellular internalization and trans-barrier trafficking of nanostructures. Int J Nanomedicine 2015;10:2191-206.
14. Yoo JW, Chambers E, Mitragotri S. Factors that control the circulation time of nanoparticles in blood: Challenges, solutions and future prospects. Curr Pharm Des 2010;16:2298-307.
15. Anbarasu M, Anandan M, Chinnasamy E. Gopinath V, Balamurugan K. Synthesis and characterizationof polyethylene glycol (PEG) coated Fe3O4 nanoparticles by chemical co-precipitation method forbiomedical applications. Spectrochim Acta A Mol Biomol Spectrosc 2015;135:536-9.
16. Cheng LC, Jiang X, Wang J, Chen C, Liu RS. Nano-bio effects: Interaction of nanomaterials with cells. Nanoscale 2013;5:3547-69.
17. Gratton SE, Ropp PA, Pohlhaus PD, Luft JC, Madden VJ, Napier ME, *et al.* The effect of particle design on cellular internalization pathways. Proc Natl Acad Sci U S A 2008;105:11613-8.
18. Decuzzi P, Ferrari M. The adhesive strength of non-spherical particles mediated by specific interactions. Biomaterials 2006;27:5307-14-22.
19. Hall E. The Physics and Chemistry of radiation absorption. In: Radiobiology for the Radiologist. 5th ed. Philadelphia, PA: Lippincott Williams and Wilkins; 2000. p. 5-16.
20. Malega F, Indrayana I, Suharyadi E. Synthesis and characterization of the microstructure and functionalgroup bond of Fe3O4 nanoparticles from natural iron sand in Tobelo North Halmahera. J Ilmiah Pendidikan Fisika Al-Biruni 2018;7:13-22.
21. Masoudi A, Hosseini HR, Shokrgozar MA, Ahmadi R, Oghabian MA. The effect of poly(ethyleneglycol) coating on colloidal stability of superparamagnetic iron oxide nanoparticles as potential MRI contrastagent. Int J Pharm 2012;433:129-41.
22. Shameli K, Ahmad MB, Jazayeri SD, Sedaghat S, Shabanzadeh P, Jahangirian H, *et al.* Synthesisand characterization of polyethylene glycolmediated silver nanoparticles by the green method. Int J Mol Sci 2012;13:6639-50.
23. Gumustas M, Sengel Turk CT, Gumustas A, Ozkan SA, Uslu B. Effect of polymer-basednanoparticles on the assay of antimicrobial drug delivery systems. In: Grumezescu AM, editor. Multifunctional Systems for Combined Delivery, Biosensing and Diagnostics. Ch. 5. Amsterdam, The Netherlands: Elsevier; 2017. p. 67-108.
24. Fonte P, Andrade F, Araújo F, Andrade C, Neves Jd, Sarmento B. Chitosan-coated solid lipid nanoparticles for insulin delivery. Methods Enzymol 2012;508:295-314.
25. Abhiram CA, Kadarkarai G, Murali R. Synthesis of poly (ethylene glycol) (PEG)-capped Fe3O4 nanoclusters by hydrothermal method. IOP Conf. Ser. Mater. Sci. Eng. 2019;577;012153.
26. Shete PB, Patil RM, Ningthoujam RS, Ghosh SJ, Pawar SH. Magnetic core shell structures formagnetic fluid hyperthermia therapy application. New J Chem 2013;37:3784-92.
27. Bañobre-López M, Teijeiro A, Rivas J. Magnetic nanoparticle-based hyperthermia for cancer treatment. Rep Pract Oncol Radiother 2013;18:397-400.
28. Brusentov NA, Gogosov VV, Brusentov TN, SergeevAV, Jurchenko NY, Kuznetsov AA, *et al*. Evaluation of ferromagnetic fluids and suspensions for the site-specific radiofrequency-induced hyperthermia of MX11 sarcoma cells in vitro. J Magn Magn Mater 2001;225:113-7.
29. Xu CJ, Xu KM, Gu HW, Zhong XF, Guo ZH, Zheng R, *et al*. Dopamine as a robust anchor to immobilize functional molecules on the iron oxide shell of magnetic nanoparticles. J Am Chem Soc 2004;126:3392-401.
30. Liu G, Li Y, Yang L, Wei Y, Wang X, Wang Z, *et al*. Cytotoxicity study of polyethylene glycolderivatives. RSC Adv 2017;7:18252-9.